Decomposition processes

acetylene and ammonia

W. Dal'Maz Silva

17th May 2016

Table of Contents

Table of Contents

Introduction

Pyrolysis
Thermochemical decomposition of organic material at high temperature in the absence of oxygen.

Heterogeneous processes
Adsorption, desorption, decomposition and recombination processes of molecules at solid surfaces.

Context
Decomposition of precursors – C_2H_2 and NH_3 – during carbonitriding treatment of low alloy steels.

Objective
Study precursors decomposition in order to control interstitial enrichment during steel carbonitriding.

Methods
Gas chromatography, diffusion profile evaluation, thermogravimetry and numerical simulation.

Introduction

Pyrolysis
Thermochemical decomposition of organic material at high temperature in the absence of oxygen.

Heterogeneous processes
Adsorption, desorption, decomposition and recombination processes of molecules at solid surfaces.

Context
Decomposition of precursors – C_2H_2 and NH_3 – during carbonitriding treatment of low alloy steels.

Objective
Study precursors decomposition in order to control interstitial enrichment during steel carbonitriding.

Methods
Gas chromatography, diffusion profile evaluation, thermogravimetry and numerical simulation.

Introduction

Pyrolysis
Thermochemical decomposition of organic material at high temperature in the absence of oxygen.

Heterogeneous processes
Adsorption, desorption, decomposition and recombination processes of molecules at solid surfaces.

Context
Decomposition of precursors – C_2H_2 and NH_3 – during carbonitriding treatment of low alloy steels.

Objective
Study precursors decomposition in order to control interstitial enrichment during steel carbonitriding.

Methods
Gas chromatography, diffusion profile evaluation, thermogravimetry and numerical simulation.

Introduction

Pyrolysis
Thermochemical decomposition of organic material at high temperature in the absence of oxygen.

Heterogeneous processes
Adsorption, desorption, decomposition and recombination processes of molecules at solid surfaces.

Context
Decomposition of precursors – C_2H_2 and NH_3 – during carbonitriding treatment of low alloy steels.

Objective
Study precursors decomposition in order to control interstitial enrichment during steel carbonitriding.

Methods
Gas chromatography, diffusion profile evaluation, thermogravimetry and numerical simulation.

Introduction

Pyrolysis
Thermochemical decomposition of organic material at high temperature in the absence of oxygen.

Heterogeneous processes
Adsorption, desorption, decomposition and recombination processes of molecules at solid surfaces.

Context
Decomposition of precursors – C_2H_2 and NH_3 – during carbonitriding treatment of low alloy steels.

Objective
Study precursors decomposition in order to control interstitial enrichment during steel carbonitriding.

Methods
Gas chromatography, diffusion profile evaluation, thermogravimetry and numerical simulation.

Table of Contents

Residence time distribution

Background

Purpose: reactor diagnosis/modelling

Reactor types: ideal vs. real

Concepts:

- residence time distribution (RTD)
- mixing behavior
- reactor model

Aim: conversion prediction

Measuring RTD:

- pulse of tracer
- step of tracer

Think!

Portions of gas injected at a given instant leave the reactor at different moments: the conversion is averaged by these times but also by the mixing of arriving species at each position.

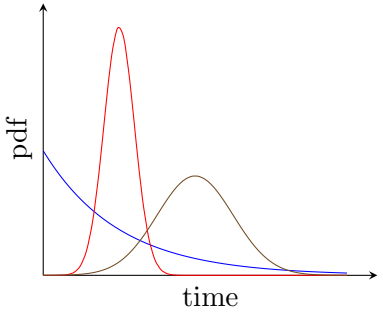

Residence time distribution

Background

Purpose: reactor diagnosis/modelling

Reactor types: ideal vs. real

Concepts:

- residence time distribution (RTD)
- mixing behavior
- reactor model

Aim: conversion prediction

Measuring RTD:

- pulse of tracer
- step of tracer

Think!

Portions of gas injected at a given instant leave the reactor at different moments: the conversion is averaged by these times but also by the mixing of arriving species at each position.

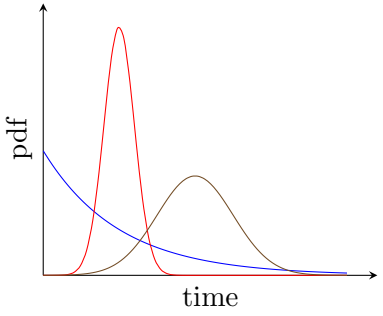

Residence time distribution

Background

Purpose: reactor diagnosis/modelling

Reactor types: ideal vs. real

Concepts:

- residence time distribution (RTD)
- mixing behavior
- reactor model

Aim: conversion prediction

Measuring RTD:

- pulse of tracer
- step of tracer

Think!

Portions of gas injected at a given instant leave the reactor at different moments: the conversion is averaged by these times but also by the mixing of arriving species at each position.

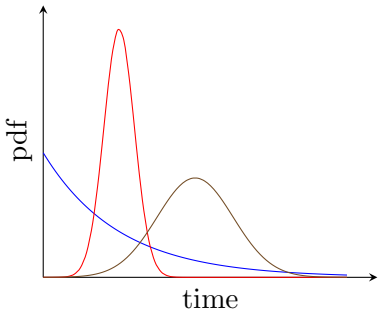

Residence time distribution

Background

Purpose: reactor diagnosis/modelling

Reactor types: ideal vs. real

Concepts:

- residence time distribution (RTD)
- mixing behavior
- reactor model

Aim: conversion prediction

Measuring RTD:

- pulse of tracer
- step of tracer

Think!

Portions of gas injected at a given instant leave the reactor at different moments: the conversion is averaged by these times but also by the mixing of arriving species at each position.

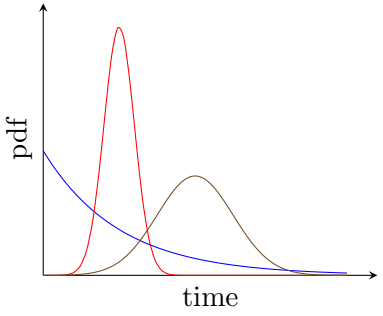

Residence time distribution

Background

Purpose: reactor diagnosis/modelling

Reactor types: ideal vs. real

Concepts:

- residence time distribution (RTD)
- mixing behavior
- reactor model

Aim: conversion prediction

Measuring RTD:

- pulse of tracer
- step of tracer

Think!

Portions of gas injected at a given instant leave the reactor at different moments: the conversion is averaged by these times but also by the mixing of arriving species at each position.

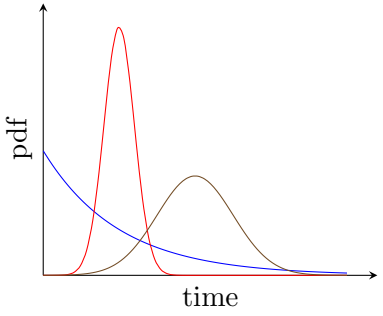

Residence time distribution

Background

Purpose: reactor diagnosis/modelling

Reactor types: ideal vs. real

Concepts:

- residence time distribution (RTD)
- mixing behavior
- reactor model

Aim: conversion prediction

Measuring RTD:

- pulse of tracer
- step of tracer

Think!

Portions of gas injected at a given instant leave the reactor at different moments: the conversion is averaged by these times but also by the mixing of arriving species at each position.

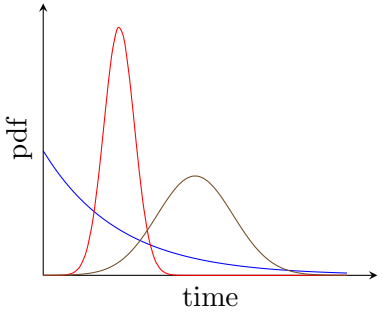

Residence time distribution

Measurements

Method: tracer (CH_4) pulse in N_2

Detection: FID (by-passing the column)

Study parameters:

- total flow rate
- heated zone temperature
- loading (with or without sample)

Bodenstein number: 5 – 10

Mixing: complete micromixing

Model: maximum mixedness

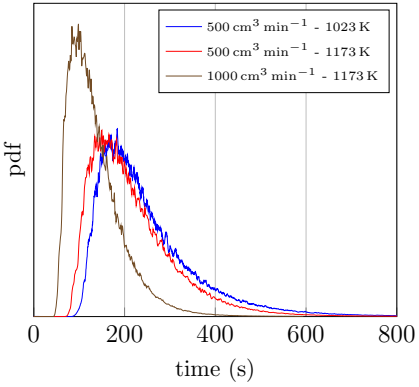

↑ flow rate $\Rightarrow \downarrow \tau \downarrow \sigma$

↑ temperature $\Rightarrow \downarrow \tau \sim \sigma$

Residence time distribution

Measurements

Method: tracer (CH_4) pulse in N_2

Detection: FID (by-passing the column)

Study parameters:

- total flow rate
- heated zone temperature
- loading (with or without sample)

Bodenstein number: 5 – 10

Mixing: complete micromixing

Model: maximum mixedness

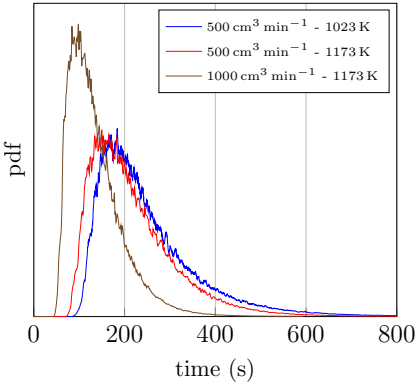

↑ flow rate $\Rightarrow \downarrow \tau \downarrow \sigma$

↑ temperature $\Rightarrow \downarrow \tau \sim \sigma$

Residence time distribution

Measurements

Method: tracer (CH_4) pulse in N_2

Detection: FID (by-passing the column)

Study parameters:

- total flow rate
- heated zone temperature
- loading (with or without sample)

Bodenstein number: 5 – 10

Mixing: complete micromixing

Model: maximum mixedness

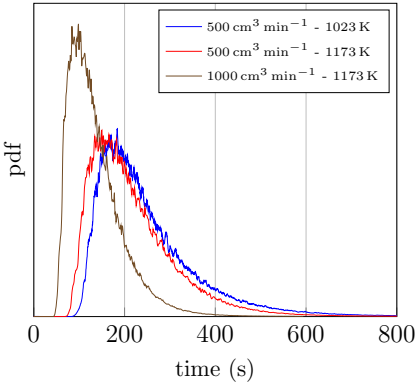

↑ flow rate $\Rightarrow \downarrow \tau \downarrow \sigma$

↑ temperature $\Rightarrow \downarrow \tau \sim \sigma$

Residence time distribution

Measurements

Method: tracer (CH_4) pulse in N_2

Detection: FID (by-passing the column)

Study parameters:

- total flow rate
- heated zone temperature
- loading (with or without sample)

Bodenstein number: 5 – 10

Mixing: complete micromixing

Model: maximum mixedness

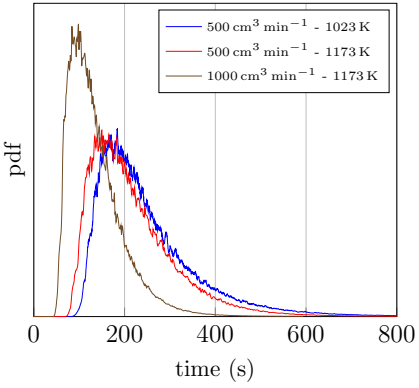

↑ flow rate $\Rightarrow \downarrow \tau \downarrow \sigma$

↑ temperature $\Rightarrow \downarrow \tau \sim \sigma$

Residence time distribution

Measurements

Method: tracer (CH_4) pulse in N_2

Detection: FID (by-passing the column)

Study parameters:

- total flow rate
- heated zone temperature
- loading (with or without sample)

Bodenstein number: 5 – 10

Mixing: complete micromixing

Model: maximum mixedness

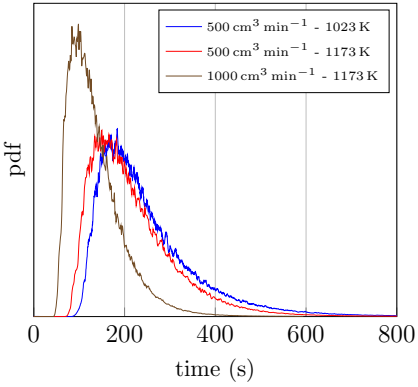

↑ flow rate $\Rightarrow \downarrow \tau \downarrow \sigma$

↑ temperature $\Rightarrow \downarrow \tau \sim \sigma$

Residence time distribution

Measurements

Method: tracer (CH_4) pulse in N_2

Detection: FID (by-passing the column)

Study parameters:

- total flow rate
- heated zone temperature
- loading (with or without sample)

Bodenstein number: 5 – 10

Mixing: complete micromixing

Model: maximum mixedness

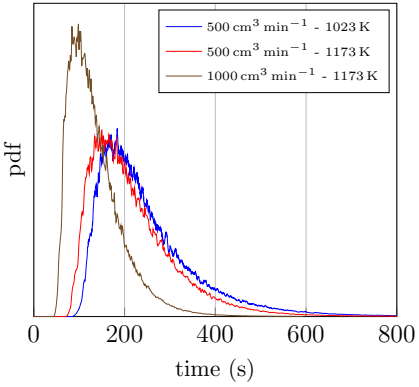

↑ flow rate $\Rightarrow \downarrow \tau \downarrow \sigma$

↑ temperature $\Rightarrow \downarrow \tau \sim \sigma$

Residence time distribution

Measurements

Method: tracer (CH_4) pulse in N_2

Detection: FID (by-passing the column)

Study parameters:

- total flow rate
- heated zone temperature
- loading (with or without sample)

Bodenstein number: 5 – 10

Mixing: complete micromixing

Model: maximum mixedness

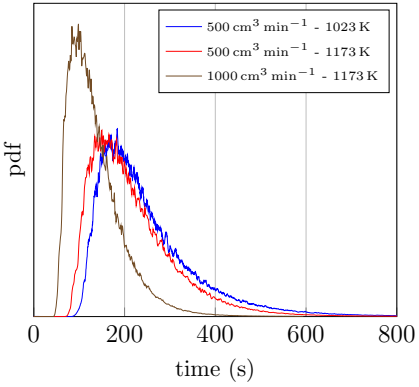

↑ flow rate $\Rightarrow \downarrow \tau \downarrow \sigma$

↑ temperature $\Rightarrow \downarrow \tau \sim \sigma$

Residence time distribution

Measurements

Method: tracer (CH_4) pulse in N_2

Detection: FID (by-passing the column)

Study parameters:

- total flow rate
- heated zone temperature
- loading (with or without sample)

Bodenstein number: 5 – 10

Mixing: complete micromixing

Model: maximum mixedness

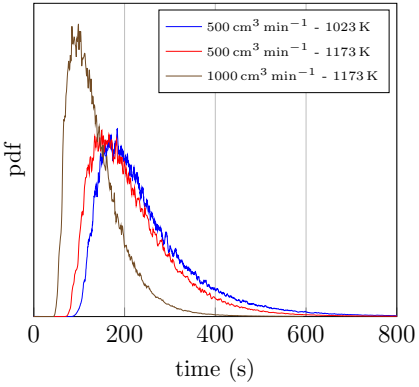

↑ flow rate $\Rightarrow \downarrow \tau \downarrow \sigma$

↑ temperature $\Rightarrow \downarrow \tau \sim \sigma$

Table of Contents

Acetylene decomposition

Atmospheric pressure

Input atmosphere: $N_2 - 0.02\,C_2H_2$

Temperature range: 823 K to 1223 K

Flow rates: 500 $cm^3\,min^{-1}$ and 1000 $cm^3\,min^{-1}$

Measured species: H_2, CH_4, C_2H_2 and C_2H_4

Observations:

- Decomposition detectable above 873 K
- Most important light-weight hydrocarbon formed below 1100 K: C_2H_4
- At 1173 K: $x(C_2H_2)$ is 5× other hydrocarbons and only 50% of the released H atoms are on H_2 molecules
- C_2H_6 is not detected unless excess H_2 is added to the input atmosphere

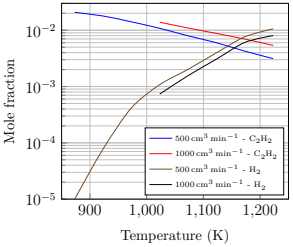

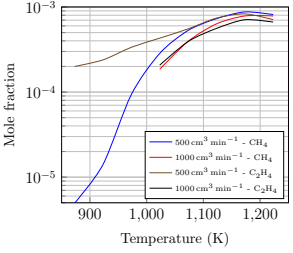

Acetylene decomposition

Atmospheric pressure

Input atmosphere: N_2 – 0.02 C_2H_2

Temperature range: 823 K to 1223 K

Flow rates: 500 $cm^3\,min^{-1}$ and 1000 $cm^3\,min^{-1}$

Measured species: H_2, CH_4, C_2H_2 and C_2H_4

Observations:

- Decomposition detectable above 873 K
- Most important light-weight hydrocarbon formed below 1100 K: C_2H_4
- At 1173 K: $x(C_2H_2)$ is 5× other hydrocarbons and only 50% of the released H atoms are on H_2 molecules
- C_2H_6 is not detected unless excess H_2 is added to the input atmosphere

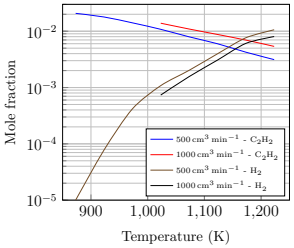

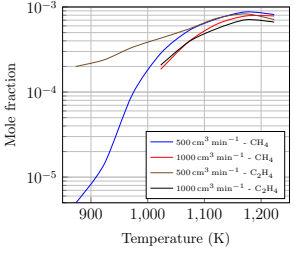

Acetylene decomposition

Atmospheric pressure

Input atmosphere: N_2 – 0.02 C_2H_2

Temperature range: 823 K to 1223 K

Flow rates: 500 $cm^3\,min^{-1}$ and 1000 $cm^3\,min^{-1}$

Measured species: H_2, CH_4, C_2H_2 and C_2H_4

Observations:

- Decomposition detectable above 873 K
- Most important light-weight hydrocarbon formed below 1100 K: C_2H_4
- At 1173 K: $x(C_2H_2)$ is 5× other hydrocarbons and only 50% of the released H atoms are on H_2 molecules
- C_2H_6 is not detected unless excess H_2 is added to the input atmosphere

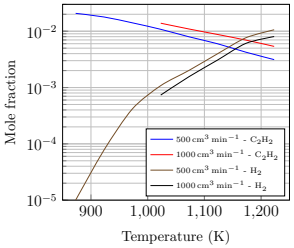

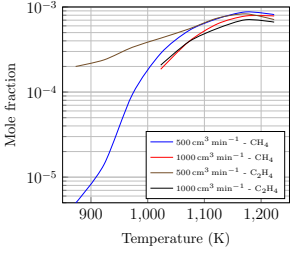

Acetylene decomposition

Atmospheric pressure

Input atmosphere: N_2 – 0.02 C_2H_2

Temperature range: 823 K to 1223 K

Flow rates: 500 $cm^3\,min^{-1}$ and 1000 $cm^3\,min^{-1}$

Measured species: H_2, CH_4, C_2H_2 and C_2H_4

Observations:

- Decomposition detectable above 873 K
- Most important light-weight hydrocarbon formed below 1100 K: C_2H_4
- At 1173 K: $x(C_2H_2)$ is 5× other hydrocarbons and only 50% of the released H atoms are on H_2 molecules
- C_2H_6 is not detected unless excess H_2 is added to the input atmosphere

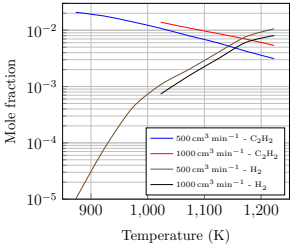

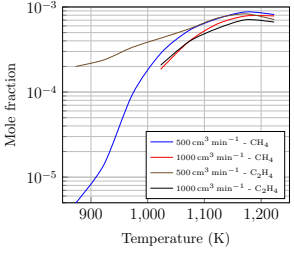

Acetylene decomposition

Atmospheric pressure

Input atmosphere: N_2 – 0.02 C_2H_2

Temperature range: 823 K to 1223 K

Flow rates: 500 $cm^3\,min^{-1}$ and 1000 $cm^3\,min^{-1}$

Measured species: H_2, CH_4, C_2H_2 and C_2H_4

Observations:

- Decomposition detectable above 873 K
- Most important light-weight hydrocarbon formed below 1100 K: C_2H_4
- At 1173 K: $x(C_2H_2)$ is 5× other hydrocarbons and only 50% of the released H atoms are on H_2 molecules
- C_2H_6 is not detected unless excess H_2 is added to the input atmosphere

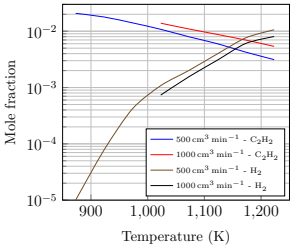

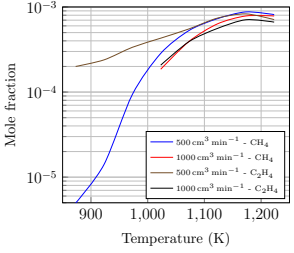

Acetylene decomposition

Atmospheric pressure

Input atmosphere: N_2 – 0.02 C_2H_2

Temperature range: 823 K to 1223 K

Flow rates: 500 $cm^3\,min^{-1}$ and 1000 $cm^3\,min^{-1}$

Measured species: H_2, CH_4, C_2H_2 and C_2H_4

Observations:

- Decomposition detectable above 873 K
- Most important light-weight hydrocarbon formed below 1100 K: C_2H_4
- At 1173 K: $x(C_2H_2)$ is 5× other hydrocarbons and only 50% of the released H atoms are on H_2 molecules
- C_2H_6 is not detected unless excess H_2 is added to the input atmosphere

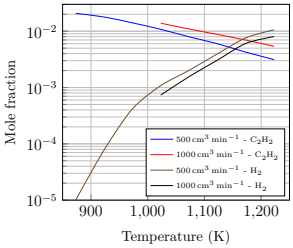

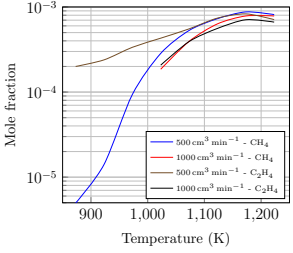

Acetylene decomposition

Atmospheric pressure

Input atmosphere: N_2 – 0.02 C_2H_2

Temperature range: 823 K to 1223 K

Flow rates: 500 $cm^3\,min^{-1}$ and 1000 $cm^3\,min^{-1}$

Measured species: H_2, CH_4, C_2H_2 and C_2H_4

Observations:

- Decomposition detectable above 873 K
- Most important light-weight hydrocarbon formed below 1100 K: C_2H_4
- At 1173 K: $x(C_2H_2)$ is 5× other hydrocarbons and only 50% of the released H atoms are on H_2 molecules
- C_2H_6 is not detected unless excess H_2 is added to the input atmosphere

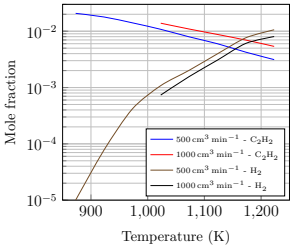

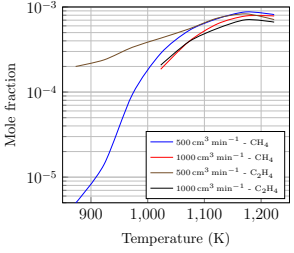

Acetylene decomposition

Atmospheric pressure

Input atmosphere: N_2 – 0.02 C_2H_2

Temperature range: 823 K to 1223 K

Flow rates: 500 $cm^3\,min^{-1}$ and 1000 $cm^3\,min^{-1}$

Measured species: H_2, CH_4, C_2H_2 and C_2H_4

Observations:

- Decomposition detectable above 873 K
- Most important light-weight hydrocarbon formed below 1100 K: C_2H_4
- At 1173 K: $x(C_2H_2)$ is 5× other hydrocarbons and only 50% of the released H atoms are on H_2 molecules
- C_2H_6 is not detected unless excess H_2 is added to the input atmosphere

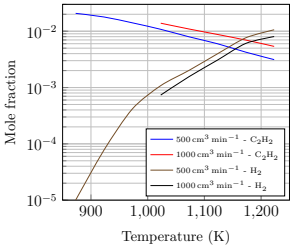

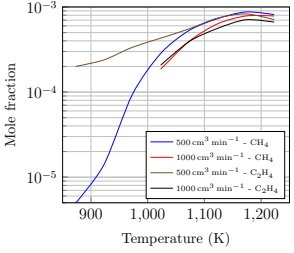

Acetylene decomposition

Atmospheric pressure: mass balance

From the previous results one may establish a mole balance for carbon and hydrogen.

Since both TCD and FID detectors were used, total and hydrocarbon H-atoms can be quantified.

An increasing ratio C/H with respect to the temperature is observed for the missing atoms: C−C bonds are prevalent over C−H bonds in the undetected species.

Given the boundary and initial conditions, C/H ratio seems independent of the flow rate: the quantity is governed by the high temperature zone in the reactor.

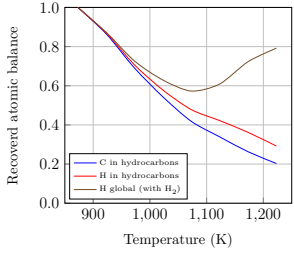

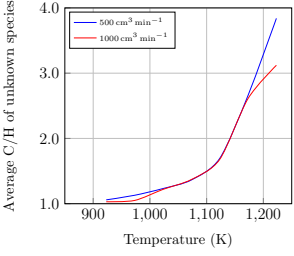

Acetylene decomposition

Atmospheric pressure: mass balance

From the previous results one may establish a mole balance for carbon and hydrogen.

Since both TCD and FID detectors were used, total and hydrocarbon H-atoms can be quantified.

An increasing ratio C/H with respect to the temperature is observed for the missing atoms: C−C bonds are prevalent over C−H bonds in the undetected species.

Given the boundary and initial conditions, C/H ratio seems independent of the flow rate: the quantity is governed by the high temperature zone in the reactor.

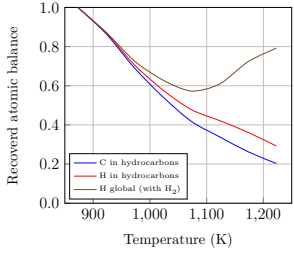

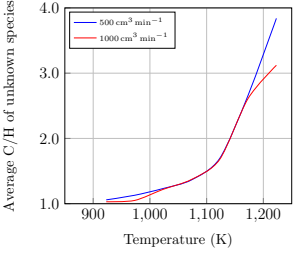

Acetylene decomposition

Atmospheric pressure: mass balance

From the previous results one may establish a mole balance for carbon and hydrogen.

Since both TCD and FID detectors were used, total and hydrocarbon H-atoms can be quantified.

An increasing ratio C/H with respect to the temperature is observed for the missing atoms: C−C bonds are prevalent over C−H bonds in the undetected species.

Given the boundary and initial conditions, C/H ratio seems independent of the flow rate: the quantity is governed by the high temperature zone in the reactor.

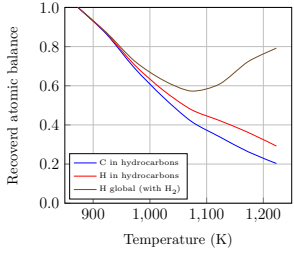

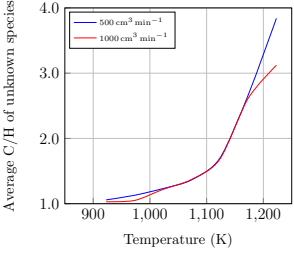

Acetylene decomposition

Atmospheric pressure: mass balance

From the previous results one may establish a mole balance for carbon and hydrogen.

Since both TCD and FID detectors were used, total and hydrocarbon H-atoms can be quantified.

An increasing ratio C/H with respect to the temperature is observed for the missing atoms: **C−C bonds are prevalent over C−H bonds in the undetected species.**

Given the boundary and initial conditions, C/H ratio seems independent of the flow rate: the quantity is governed by the high temperature zone in the reactor.

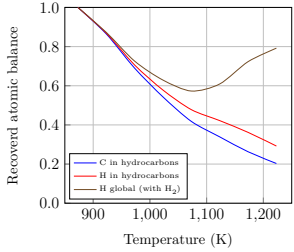

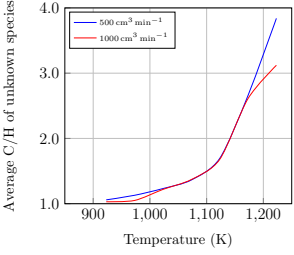

Acetylene decomposition

Atmospheric pressure: mass balance

From the previous results one may establish a mole balance for carbon and hydrogen.

Since both TCD and FID detectors were used, total and hydrocarbon H-atoms can be quantified.

An increasing ratio C/H with respect to the temperature is observed for the missing atoms: C−C bonds are prevalent over C−H bonds in the undetected species.

Given the boundary and initial conditions, C/H ratio seems independent of the flow rate: the quantity is governed by the high temperature zone in the reactor.

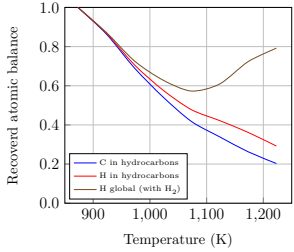

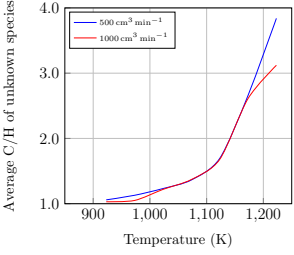

Acetylene decomposition

Atmospheric pressure: mass balance

From the previous results one may establish a mole balance for carbon and hydrogen.

Since both TCD and FID detectors were used, total and hydrocarbon H-atoms can be quantified.

An increasing ratio C/H with respect to the temperature is observed for the missing atoms: C−C bonds are prevalent over C−H bonds in the undetected species.

Given the boundary and initial conditions, C/H ratio seems independent of the flow rate: **the quantity is governed by the high temperature zone in the reactor.**

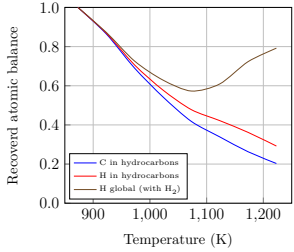

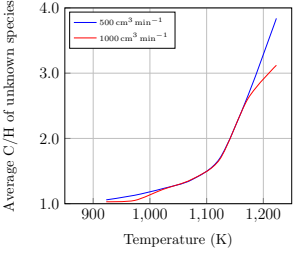

Acetylene decomposition

Atmospheric pressure: carburizing

Input atmosphere: $N_2 - 0.01\,C_2H_2$

Temperature: 1173 K

Flow rate: $500\,cm^3\,min^{-1}$

Observations:

- Metallic sample does not interfere in the order of magnitude of the observed hydrocarbons
- Good agreement between simulation and mass intake for a constant concentration boundary condition
- Even partial pressures below 5 mbar are enough for surface saturation

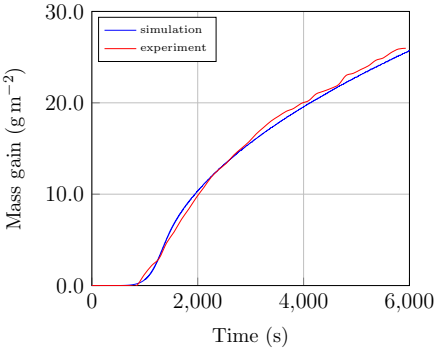

Acetylene decomposition

Atmospheric pressure: carburizing

Input atmosphere: $N_2 - 0.01\,C_2H_2$

Temperature: 1173 K

Flow rate: $500\,cm^3\,min^{-1}$

Observations:

- Metallic sample does not interfere in the order of magnitude of the observed hydrocarbons
- Good agreement between simulation and mass intake for a constant concentration boundary condition
- Even partial pressures below 5 mbar are enough for surface saturation

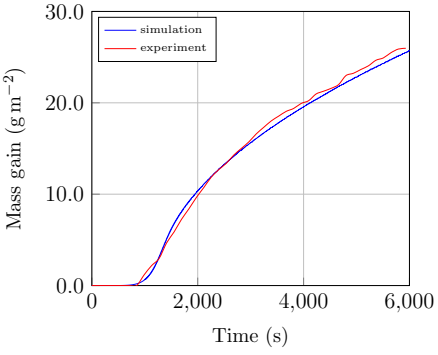

Acetylene decomposition

Atmospheric pressure: carburizing

Input atmosphere: $N_2 - 0.01\,C_2H_2$

Temperature: 1173 K

Flow rate: $500\,cm^3\,min^{-1}$

Observations:

- Metallic sample does not interfere in the order of magnitude of the observed hydrocarbons
- Good agreement between simulation and mass intake for a constant concentration boundary condition
- Even partial pressures below 5 mbar are enough for surface saturation

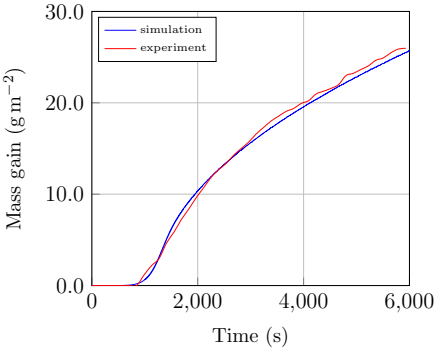

Acetylene decomposition

Atmospheric pressure: carburizing

Input atmosphere: $N_2 - 0.01\,C_2H_2$

Temperature: $1173\,K$

Flow rate: $500\,cm^3\,min^{-1}$

Observations:

- Metallic sample does not interfere in the order of magnitude of the observed hydrocarbons
- Good agreement between simulation and mass intake for a constant concentration boundary condition
- Even partial pressures below 5 mbar are enough for surface saturation

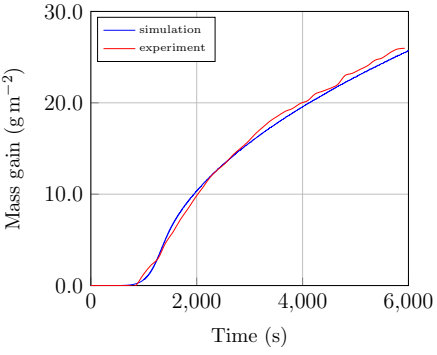

Acetylene decomposition

Atmospheric pressure: carburizing

Input atmosphere: $N_2 - 0.01\,C_2H_2$

Temperature: $1173\,K$

Flow rate: $500\,cm^3\,min^{-1}$

Observations:

- Metallic sample does not interfere in the order of magnitude of the observed hydrocarbons
- Good agreement between simulation and mass intake for a constant concentration boundary condition
- Even partial pressures below 5 mbar are enough for surface saturation

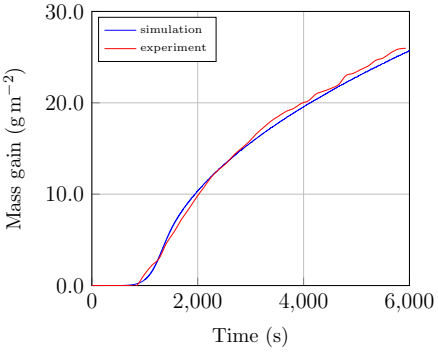

Acetylene decomposition

Atmospheric pressure: carburizing

Input atmosphere: $N_2 - 0.01\,C_2H_2$

Temperature: 1173 K

Flow rate: $500\,cm^3\,min^{-1}$

Observations:

- Metallic sample does not interfere in the order of magnitude of the observed hydrocarbons
- Good agreement between simulation and mass intake for a constant concentration boundary condition
- Even partial pressures below 5 mbar are enough for surface saturation

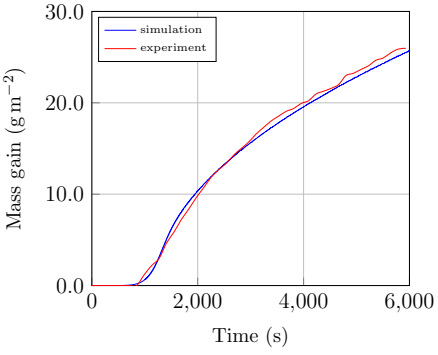

Using global rate parameters $k = 1.5$ and $n = 2.7$ for acetylene pyrolysis[1] coupled to experimental RTD functions with maximum mixedness model

$$\frac{\mathrm{d}c_i}{\mathrm{d}t} = -\left[kc_i^n + (c_i - c_{i,0})\frac{E(t_{max} - t)}{1 - F(t_{max} - t)}\right]$$

the following predictions are made (given in mole fractions):

Flow ($\mathrm{cm^3\,min^{-1}}$)	Measured $\times 10^3$	Simulated $\times 10^3$	Ratio
250	3.67	3.01	0.82
500	4.25	4.18	0.98
1000	6.96	5.54	0.80

[1] Norinaga et al. Carbon 44 (2006) 1790–1800.

Acetylene decomposition

Pyrolysis mechanism

Kinetic mechanism:

- Norinaga et al. J. Anal. Appl. Pyrolysis 86 (2009) 148-160
- 241 species (nodes)
- 902 reactions
- 1933 undirected edges

Analyses:

- Simplification using DRG method
- System conditioning through interaction ordering
- Maximum mixedness solution of complete and simplified systems

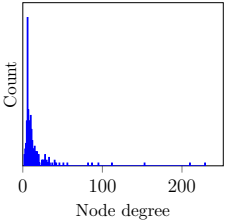

Species	Degree
H	229
H_2	210
C_2H_2	153
CH_3	112
CH_4	95
C_2H_3	87
C_2H_4	82
C_6H_6	56
C_6H_5	51
C_4H_4	46

Acetylene decomposition

Pyrolysis mechanism

Kinetic mechanism:

- Norinaga et al. J. Anal. Appl. Pyrolysis 86 (2009) 148-160
- 241 species (nodes)
- 902 reactions
- 1933 undirected edges

Analyses:

- Simplification using DRG method
- System conditioning through interaction ordering
- Maximum mixedness solution of complete and simplified systems

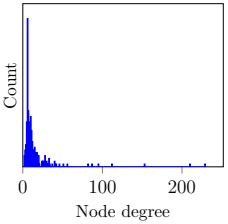

Species	Degree
H	229
H_2	210
C_2H_2	153
CH_3	112
CH_4	95
C_2H_3	87
C_2H_4	82
C_6H_6	56
C_6H_5	51
C_4H_4	46

Acetylene decomposition

Pyrolysis mechanism

Kinetic mechanism:

- Norinaga et al. J. Anal. Appl. Pyrolysis 86 (2009) 148-160
- 241 species (nodes)
- 902 reactions
- 1933 undirected edges

Analyses:

- Simplification using DRG method
- System conditioning through interaction ordering
- Maximum mixedness solution of complete and simplified systems

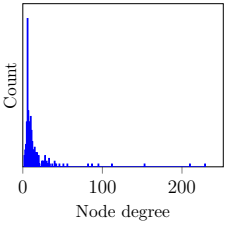

Species	Degree
H	229
H_2	210
C_2H_2	153
CH_3	112
CH_4	95
C_2H_3	87
C_2H_4	82
C_6H_6	56
C_6H_5	51
C_4H_4	46

Acetylene decomposition

Pyrolysis mechanism

Kinetic mechanism:

- Norinaga et al. J. Anal. Appl. Pyrolysis 86 (2009) 148-160
- 241 species (nodes)
- 902 reactions
- 1933 undirected edges

Analyses:

- Simplification using DRG method
- System conditioning through interaction ordering
- Maximum mixedness solution of complete and simplified systems

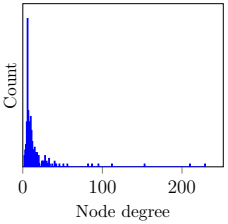

Species	Degree
H	229
H_2	210
C_2H_2	153
CH_3	112
CH_4	95
C_2H_3	87
C_2H_4	82
C_6H_6	56
C_6H_5	51
C_4H_4	46

Acetylene decomposition

Pyrolysis mechanism

Kinetic mechanism:

- Norinaga et al. J. Anal. Appl. Pyrolysis 86 (2009) 148-160
- 241 species (nodes)
- 902 reactions
- 1933 undirected edges

Analyses:

- Simplification using DRG method
- System conditioning through interaction ordering
- Maximum mixedness solution of complete and simplified systems

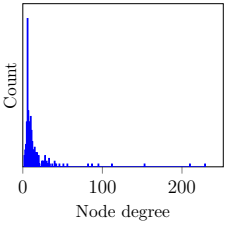

Species	Degree
H	229
H_2	210
C_2H_2	153
CH_3	112
CH_4	95
C_2H_3	87
C_2H_4	82
C_6H_6	56
C_6H_5	51
C_4H_4	46

Acetylene decomposition

Pyrolysis mechanism

Kinetic mechanism:

- Norinaga et al. J. Anal. Appl. Pyrolysis 86 (2009) 148-160
- 241 species (nodes)
- 902 reactions
- 1933 undirected edges

Analyses:

- Simplification using DRG method
- System conditioning through interaction ordering
- Maximum mixedness solution of complete and simplified systems

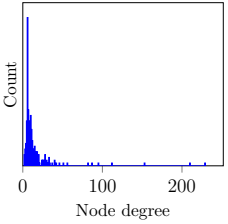

Species	Degree
H	229
H_2	210
C_2H_2	153
CH_3	112
CH_4	95
C_2H_3	87
C_2H_4	82
C_6H_6	56
C_6H_5	51
C_4H_4	46

Acetylene decomposition

Pyrolysis mechanism

Kinetic mechanism:

- Norinaga et al. J. Anal. Appl. Pyrolysis 86 (2009) 148-160
- 241 species (nodes)
- 902 reactions
- 1933 undirected edges

Analyses:

- Simplification using DRG method
- System conditioning through interaction ordering
- Maximum mixedness solution of complete and simplified systems

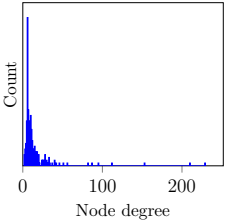

Species	Degree
H	229
H_2	210
C_2H_2	153
CH_3	112
CH_4	95
C_2H_3	87
C_2H_4	82
C_6H_6	56
C_6H_5	51
C_4H_4	46

Acetylene decomposition

Pyrolysis mechanism

Kinetic mechanism:

- Norinaga et al. J. Anal. Appl. Pyrolysis 86 (2009) 148-160
- 241 species (nodes)
- 902 reactions
- 1933 undirected edges

Analyses:

- Simplification using DRG method
- System conditioning through interaction ordering
- Maximum mixedness solution of complete and simplified systems

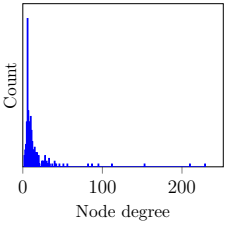

Species	Degree
H	229
H_2	210
C_2H_2	153
CH_3	112
CH_4	95
C_2H_3	87
C_2H_4	82
C_6H_6	56
C_6H_5	51
C_4H_4	46

Table of Contents

Ammonia decomposition

Pressure: 1 bar

Temperature range: 773 K to 1223 K

Flow rate: 415 $cm^3\,min^{-1}$

Atmosphere: 0.24 N_2 – 0.72 H_2 – 0.04 NH_3

Observations:

- Decomposition break-through above 950 K
- Less than 10% of initial ammonia is reminiscent at carbonitriding temperatures

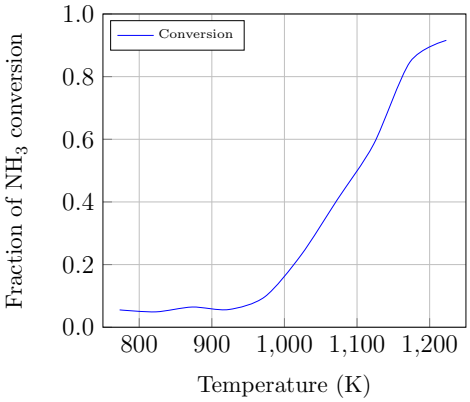

Ammonia decomposition

Pressure: 1 bar

Temperature range: 773 K to 1223 K

Flow rate: 415 $cm^3\,min^{-1}$

Atmosphere: 0.24 N_2 – 0.72 H_2 – 0.04 NH_3

Observations:

- Decomposition break-through above 950 K
- Less than 10% of initial ammonia is reminiscent at carbonitriding temperatures

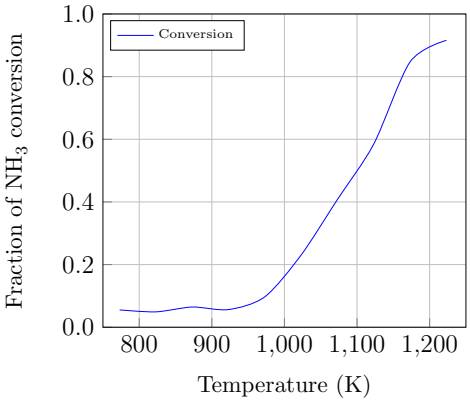

Ammonia decomposition

Pressure: 1 bar

Temperature range: 773 K to 1223 K

Flow rate: 415 $cm^3\,min^{-1}$

Atmosphere: 0.24 N_2 – 0.72 H_2 – 0.04 NH_3

Observations:

- Decomposition break-through above 950 K
- Less than 10% of initial ammonia is reminiscent at carbonitriding temperatures

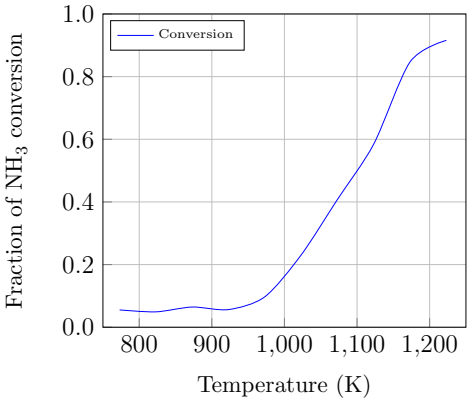

Ammonia decomposition

Pressure: 1 bar

Temperature range: 773 K to 1223 K

Flow rate: 415 $cm^3\,min^{-1}$

Atmosphere: $0.24\,N_2 - 0.72\,H_2 - 0.04\,NH_3$

Observations:

- Decomposition break-through above 950 K
- Less than 10% of initial ammonia is reminiscent at carbonitriding temperatures

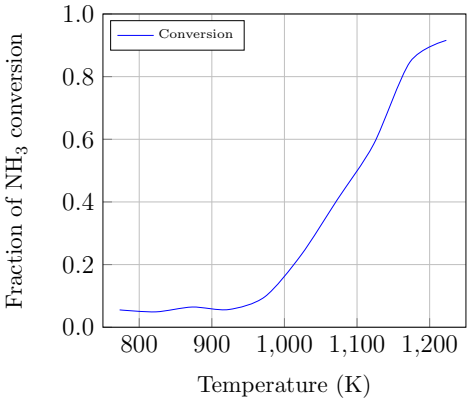

Ammonia decomposition

Pressure: 1 bar

Temperature range: 773 K to 1223 K

Flow rate: 415 $cm^3\,min^{-1}$

Atmosphere: 0.24 N_2 – 0.72 H_2 – 0.04 NH_3

Observations:

- Decomposition break-through above 950 K
- Less than 10% of initial ammonia is reminiscent at carbonitriding temperatures

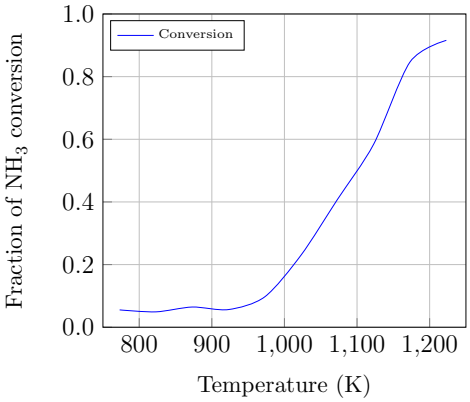

Ammonia decomposition

Pressure: 1 bar

Temperature range: 773 K to 1223 K

Flow rate: 415 $cm^3\,min^{-1}$

Atmosphere: 0.24 N_2 − 0.72 H_2 − 0.04 NH_3

Observations:

- Decomposition break-through above 950 K
- Less than 10% of initial ammonia is reminiscent at carbonitriding temperatures

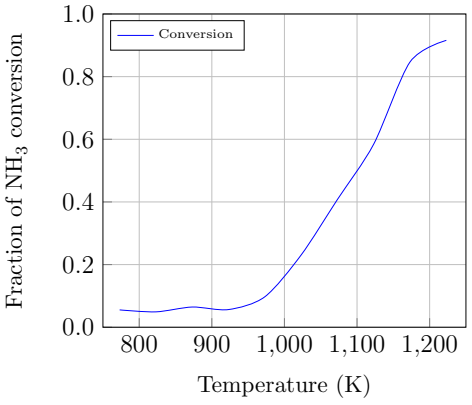

Table of Contents

Ongoing studies

Low pressure admission control for gas chromatography currently operating above 30 mbar.

Reliable measurements of C_2H_2 and NH_3 decomposition are currently being held.

Semi-automate system simplification routine for CFD simulations is under improvement.

Development of graph approach (pre-conditioning) to reduce stiffness of kinetic Jacobian.

Estimation of kinetic data from carburizing studies is being conducted.

Ongoing studies

Low pressure admission control for gas chromatography currently operating above 30 mbar.

Reliable measurements of C_2H_2 and NH_3 decomposition are currently being held.

Semi-automate system simplification routine for CFD simulations is under improvement.

Development of graph approach (pre-conditioning) to reduce stiffness of kinetic Jacobian.

Estimation of kinetic data from carburizing studies is being conducted.

Ongoing studies

Low pressure admission control for gas chromatography currently operating above 30 mbar.

Reliable measurements of C_2H_2 and NH_3 decomposition are currently being held.

Semi-automate system simplification routine for CFD simulations is under improvement.

Development of graph approach (pre-conditioning) to reduce stiffness of kinetic Jacobian.

Estimation of kinetic data from carburizing studies is being conducted.

Ongoing studies

Low pressure admission control for gas chromatography currently operating above 30 mbar.

Reliable measurements of C_2H_2 and NH_3 decomposition are currently being held.

Semi-automate system simplification routine for CFD simulations is under improvement.

Development of graph approach (pre-conditioning) to reduce stiffness of kinetic Jacobian.

Estimation of kinetic data from carburizing studies is being conducted.

Ongoing studies

Low pressure admission control for gas chromatography currently operating above 30 mbar.

Reliable measurements of C_2H_2 and NH_3 decomposition are currently being held.

Semi-automate system simplification routine for CFD simulations is under improvement.

Development of graph approach (pre-conditioning) to reduce stiffness of kinetic Jacobian.

Estimation of kinetic data from carburizing studies is being conducted.

Table of Contents

Conclusion

Decomposition of C_2H_2 leads to the formation of CH_4, C_2H_4 and H_2; C_2H_6 is observed under excess H_2.

Undetected species: C/H-ratio larger than unity, i.e. unsaturated character at intermediate levels (1-3) and the formation of soot (above 3).

System characterization (RTD) allowed the estimation of acetylene decomposition by using global rate parameters.

Graph analyses seem coherent with literature results[2] and allow the simplification of system kinetics for CFD simulations.

At atmospheric pressure austenitic nitriding conditions less than 10% of the injected ammonia is available to provide nitrogen to the material.

[2] F. Graf, PhD Thesis

Conclusion

Decomposition of C_2H_2 leads to the formation of CH_4, C_2H_4 and H_2; C_2H_6 is observed under excess H_2.

Undetected species: C/H-ratio larger than unity, i.e. unsaturated character at intermediate levels (1-3) and the formation of soot (above 3).

System characterization (RTD) allowed the estimation of acetylene decomposition by using global rate parameters.

Graph analyses seem coherent with literature results[2] and allow the simplification of system kinetics for CFD simulations.

At atmospheric pressure austenitic nitriding conditions less than 10% of the injected ammonia is available to provide nitrogen to the material.

[2] F. Graf, PhD Thesis

Conclusion

Decomposition of C_2H_2 leads to the formation of CH_4, C_2H_4 and H_2; C_2H_6 is observed under excess H_2.

Undetected species: C/H-ratio larger than unity, i.e. unsaturated character at intermediate levels (1-3) and the formation of soot (above 3).

System characterization (RTD) allowed the estimation of acetylene decomposition by using global rate parameters.

Graph analyses seem coherent with literature results[2] and allow the simplification of system kinetics for CFD simulations.

At atmospheric pressure austenitic nitriding conditions less than 10% of the injected ammonia is available to provide nitrogen to the material.

[2] F. Graf, PhD Thesis

Conclusion

Decomposition of C_2H_2 leads to the formation of CH_4, C_2H_4 and H_2; C_2H_6 is observed under excess H_2.

Undetected species: C/H-ratio larger than unity, i.e. unsaturated character at intermediate levels (1-3) and the formation of soot (above 3).

System characterization (RTD) allowed the estimation of acetylene decomposition by using global rate parameters.

Graph analyses seem coherent with literature results[2] and allow the simplification of system kinetics for CFD simulations.

At atmospheric pressure austenitic nitriding conditions less than 10% of the injected ammonia is available to provide nitrogen to the material.

[2] F. Graf, PhD Thesis

Conclusion

Decomposition of C_2H_2 leads to the formation of CH_4, C_2H_4 and H_2; C_2H_6 is observed under excess H_2.

Undetected species: C/H-ratio larger than unity, i.e. unsaturated character at intermediate levels (1-3) and the formation of soot (above 3).

System characterization (RTD) allowed the estimation of acetylene decomposition by using global rate parameters.

Graph analyses seem coherent with literature results[2] and allow the simplification of system kinetics for CFD simulations.

At atmospheric pressure austenitic nitriding conditions less than 10% of the injected ammonia is available to provide nitrogen to the material.

[2] F. Graf, PhD Thesis

Thanks for your attention!